Article

Not peer-reviewed version

HIV-Induced Modulation of TREM2 Expression Is Reversed by Cannabidiol: Implications for Age-Related Neuropathogenesis in People with HIV

Bryant Avalos , Jacqueline R Kulbe , Mary Ford , Anna Elizabeth Laird , Kyle Walter , Michael Mante , Jazmin Florio , Ali Boustani , Antoine Chaillon , Johannes Schlachetzki , Erin Sundermann , David Volsky , Robert A Rissman , Ronald Ellis , Scott Letendre , Jennifer Iudicello , Jerel Adam Fields *

Posted Date: 13 August 2024

doi: 10.20944/preprints202408.0904.v1

Keywords: TREM2; HIV; neuroinflammation; cannabis; immunomodulatory; CBD

 doi:10.20944/preprints202408.0904.v1

Article

HIV-Induced Modulation of TREM2 Expression Is Reversed by Cannabidiol: Implications for Age-Related Neuropathogenesis in People with HIV

Bryant Avalos, Jacqueline R Kulbe, Mary Ford, Anna Laird, Kyle Walter, Michael Mante, Jazmin Florio, Ali Boustani, Antoine Chaillon, Johannes Schlachetzki, Erin Sundermann, David Volsky, Robert Rissman, Ronald J. Ellis, Scott Letendre, Jennifer Iudicello and Jerel Adam Fields *

Department of Psychiatry, University of California, San Diego, 9500 Gilman Dr., La Jolla, CA, 92093, USA
* Correspondence: Jerel Adam Fields, Ph.D., 9500 Gilman Dr., La Jolla, CA, 92093; phone: 858-220-8249; jafields@health.ucsd.edu, Bryant Avalos, PhD: bavalosleyva@ghealth.ucsd.edu

Abstract: (1) Background: Triggering receptor expressed on myeloid cells 2 (TREM2) is involved in neuroinflammation and HIV-associated neurocognitive impairment (NCI). People with HIV (PWH) using cannabis exhibit lower inflammation and neurological disorders. We hypothesized TREM2 dysfunction mediates HIV neuropathogenesis and can be reversed by cannabinoids. **(2) Methods:** EcoHIV-infected wildtype (WT) and TREM2^{R47H} mutant mice were used to study HIV's impact on TREM2 and behavior. TREM2 and related gene expressions were examined in monocyte-derived macrophages (MDMs) from PWH (n=42) and people without HIV (PWoH; n=19) with varying cannabis use via RNA sequencing and qPCR. Differences in membrane-bound and soluble TREM2 (sTREM2) were evaluated using immunocytochemistry (ICC) and ELISA. **(3) Results:** EcoHIV increased immature and C-terminal fragment forms of TREM2 in WT mice but not in TREM2^{R47H} mice, with increased IBA1 protein in TREM2^{R47H} hippocampi, correlating with worse memory test performance. TREM2 mRNA levels increased with age in PWoH but not PWH. Cannabidiol (CBD) treatment increased TREM2 mRNA alone and with IL1β. RNA-seq showed upregulation of TREM2-related transcripts in cannabis-using PWH compared to naïve controls. IL1β increased sTREM2 and reduced membrane-bound TREM2, effects partially reversed by CBD. **(4) Conclusions:** These findings suggest HIV affects TREM2 expression modulated by cannabis and CBD, offering insights for therapeutic strategies.

Keywords: TREM2; HIV; neuroinflammation; cannabis; immunomodulatory; CBD

1. Introduction

People with HIV (PWH) continue to experience neurological disorders even with the widespread implementation of suppressive antiretroviral therapy (ART). Despite the therapeutic success of ART in PWH, HIV-associated neuroinflammation can persist and contribute to neurocognitive impairment (NCI). Current estimates of PWH with comorbid HIV-associated neurocognitive impairment (NCI) range from 20% to greater than 50% in some countries [1–3]. The Center for Disease Control and Prevention (CDC) recently estimated that over 53% of PWH in the United States were aged 50 and older [4]. As such, PWH are susceptible to NCI as well as age-related neurological disorders, including deficits in learning, memory, attention, executive function, and motor skills [5,6]. Evidence of premature aging in PWH also includes abnormalities in white matter, increased levels of β-amyloid, mitochondrial dysfunction, reactive astrocytes and microgliosis [7]. Given the high prevalence of NCI, and increased age of the population of PWH, novel in vivo, in vitro and ex vivo models are needed to provide mechanistic insights and to test therapeutic strategies.

Brain macrophages are major contributors to the chronic neuroinflammation in HIV infection and aging [8,9], and they populate the brain as three distinct cell types: microglia, perivascular

 doi:10.20944/preprints202408.0904.v1

macrophages, and monocyte-derived macrophages (MDMs)[10]. Microglia and perivascular macrophages are resident in the parenchyma of the brain, whereas MDMs traverses the blood-brain-barrier and enter the brain during disease states including early during HIV infection [10,11]. Models for HIV-induced neurotoxicity, including the novel EcoHIV murine model [12], indicate that proinflammatory brain macrophages are implicated in the neuropathogenesis of HIV [13,14]. Brain macrophages also contribute to homeostasis by modulating the inflammatory signaling and phagocytosing extracellular protein aggregates such as beta-amyloid and dying neurons, processes that may be disrupted in brains of PWH especially in those of increased age [15–19]. Brain macrophages produce and respond to cytokines that promote inflammation and can contribute to neuronal injury and apoptosis, including the pro-inflammatory cytokine interleukin-1 beta (IL-1β), which is associated with neurotoxicity in PWH and in aging related neurodegenerative diseases [20]. Thus, dampening the pro-inflammatory response of macrophages may provide potential therapeutic avenues to restore tissue homeostasis in the aging or HIV-infected brain.

Triggering receptor expressed on myeloid cells 2 (TREM2) is an immunomodulatory receptor expressed by brain macrophages and is pivotal in maintaining homeostasis in the brain [21]. TREM2 plays a key role in inflammation by promoting phagocytosis, modulating inflammatory gene expression, and suppressing inflammatory signaling pathways [22–24]. Additionally, TREM2 is involved in the recognition and clearance of dying neurons and protein aggregates such as Aβ[21,25–35], both of which are associated with HIV-associated neurocognitive impairment and Alzheimer's Disease (AD) [17,36–40]. Soluble TREM2 (sTREM2), generated through the proteolytic cleavage of membrane-bound TREM2 by proteases such as ADAM10 and ADAM17, can act as a biomarker of microglial activation and neuroinflammation [41]. Cleavage of TREM2 also results in the generation of C-terminal fragment [42]. Abnormal expression of TREM2 and sTREM2 have been observed in the cerebrospinal fluid (CSF) and plasma of individuals with various neurodegenerative diseases, including AD and multiple sclerosis [43–45]. Moreover, the TREM2 R47H gene variant, a single nucleotide polymorphism that results in an amino acid substitution at position 47, is a loss-of-function mutation that has also been associated with an increased risk of developing AD [46,47]. Individuals with the TREM2 R47H mutation may experience more severe neuroinflammatory responses in the presence of HIV, potentially leading to a higher risk of developing HAND and other neurocognitive impairments [48]. Thus, understanding the function and regulation of TREM2, including in the context of the R47H mutation, is crucial for developing therapeutic strategies for both aging-related neurodegenerative diseases and HIV-associated neurocognitive impairment.

Cannabis use in PWH has previously shown therapeutical potential in managing HIV-associated complications [49]. Recent studies have reported that PWH using cannabis have less immune cell activation compared to PWH that do not use cannabis [50,51]. Cannabis use in PWH is also associated with reduced inflammatory biomarkers in circulation [52], decreased viral DNA found in tissues [53], and a lower prevalence of neurocognitive impairment [54,55]. Delta-9-tetrahydrocannabinol (THC) and cannabidiol (CBD) are cannabinoids found in cannabis that have demonstrated promising anti-inflammatory properties crucial for managing neuroinflammation linked to neurodegenerative diseases [56,57]. CBD, known for lacking the psychoactive properties of THC, is particularly associated with significant anti-inflammatory effects by modulating the immune response to reduce inflammation and protect neural tissue from damage [58,59]. Additionally, activation of the cannabinoid type-2 receptor (CB2) on macrophages can reduce the production of pro-inflammatory cytokines while also promoting the release of anti-inflammatory molecules [60]. Targeting cannabinoid receptor 2 (CB2) on peripheral immune cells may reduce the inflammatory mechanisms implicated in HAND, suggesting a pathway for therapeutic intervention [61]. However, the precise pathways that mediate the anti-inflammatory and neuroprotective effect of cannabinoids is not fully understood, particularly in the context of PWH that use cannabis while on suppressive ART.

We hypothesized that cannabinoids like CBD promote TREM2 pathway signaling and that cannabis use in PWH can reverse the TREM2 dysfunction that mediates HIV neuropathogenesis. To begin investigation on the effect of HIV on TREM2 signaling, we used novel in vivo murine models. This is the first study to combine EcoHIV with the aging-related TREM2 R47H ($TREM2^{R47H}$) mutant

 doi:10.20944/preprints202408.0904.v1

mouse model. This study is also the first of its kind to investigate the role of TREM2 in MDMs generated from a cohort of PWH with variable cannabis-use patterns. We examined whether HIV induces alterations in TREM2 and related gene expression and assessed the impact of cannabis use and cannabinoids on TREM2-related changes. The findings presented here reveal that HIV affects TREM2 signaling and this is modulated by cannabis use, opening up much needed new avenues for therapeutic targeting in PWH on ART.

2. Materials and Methods

2.1. Ethics

Animal studies were conducted in certified animal research facilities at the University of California, San Diego. These studies also abide by the animal care guidelines set in place by the Institutional Animal Care and Use Committee (IACUC; #S02221) with full compliance with NIH guidelines. Informed written consent was obtained from all participants of this study in compliance with the Institutional Review Board (IRB; #080323) approval at the University of California, San Diego.

2.2. Animals and Treatments

To determine if HIV infection induces learning and memory deficits in mice with the TREM2 R47H gene mutation, we utilized 11-12 month-old C57BL/6 wildtype (WT) and mutant TREM2^{R47H} mice that were inoculated with saline (vehicle control) or EcoHIV (2.0 μg p24/mouse) via intraperitoneal (IP) injection. Behavioral testing was performed 4 weeks after treatment of all animals (total of 23 mice; n=5-6 per condition) and brain tissues were collected after completion of behavior tests. Total Activity Memory (TAM) testing was performed using a high-density Kinder Smart Frame cage rack system (Kinder Scientific, Poway, CA), which continuously monitors the animal's location in X, Y, Z coordinate space within the chamber using a 7x5 beam configuration. On the day of testing, animals are transported in their home cages to the behavioral testing room for acclimation. Duration of test sessions was 10 minutes and all animals were tested for three consecutive days during the habituation phase, which was followed by a 72 hour gap before the final day of testing.

2.3. Western Blot Detection of TREM2

Mouse brain tissues were processed for TREM2 immunoblotting as previously described [48]. Briefly, frontal cortex tissues from mouse brains (100 μg) were sonicated in lysis buffer (1.0 mM HEPES, 5.0 mM benzamidine, 2.0 mM β-mercaptoethanol, 3.0 mM EDTA, 0.5 mM magnesium sulfate, 0.05% sodium azide, pH 8.8) containing phosphatase inhibitor (Millipore; #524624) and protease inhibitor (Roche, #04693116001) cocktails. Samples were centrifuged at 2000 rpm at 4°C for 5 minutes before collection of supernatant containing whole lysates. Quantification of protein was conducted using a PierceTM Bicinchoninic Acid (BCA) Protein assay kit (Thermo Scientific; #23225). Protein lysates in 1X Laemmli Sample Buffer (Bio-Rad; #1610747) were vortexed, spun down, and incubated in a hot water bath at 95°C for 5 minutes. Samples were then loaded (15 μg protein per well) onto a 4–15 % CriterionTM TGX Stain-Free Protein Gel (Bio-Rad; #5678085) and electrophoresed at 200V for 45 minutes in Tris/Glycine/SDS running buffer (Bio-Rad; #1610772). Protein gels were transferred using the Trans-Blot Turbo Transfer System that includes PVDF membranes, transfer stacks, and transfer buffer from a Trans-Blot Turbo RTA transfer kit (Bio-Rad; #1704272). Gels were rinsed with water before imaging for total protein using a stain-free blot settings on a Bio-Rad ChemiDoc imager. Membranes were placed in 1X TBS 1% Casein Blocking Buffer (Bio-Rad; #1610782) for one hour at room temperature before overnight incubation at 4°C with primary antibody for rabbit anti-TREM2 (Thermo Scientific; #PA5-87933; 1:1000). Following removal of primary antibody, blots were washed in 1X PBS for 5 minutes before adding HRP-conjugated Goat Anti-Rabbit IgG secondary antibody (Bio-Rad; #1706515; 1:5000) for 1 hour at room temperature. SuperSignal® West Femto enhanced chemiluminescent substrate (Thermo Scientific; #TG26840A) was applied for visualization of protein bands on membranes. The blots were then stripped using Western Blot

 doi:10.20944/preprints202408.0904.v1

Stripping Buffer (Thermo Scientific; #21059) and re-probed with a mouse monoclonal antibody against β-actin (ACTB; Sigma-Aldrich; #A5316; 1:2000) as a loading control. Images were captured, and semi-quantitative analysis was performed on Image Lab Software (Bio-Rad v6.1).

2.4. Immunohistochemistry of Brain Sections

To determine if HIV infection affects levels of microgliosis and astrogliosis, mouse brains were collected immediately after behavioral analyses and fixed in 4% paraformaldehyde for 5 days before being sectioned and immunostained. Free-floating 40 μm thick vibratome sections of mouse brains were washed with phosphate-buffered saline with Tween 20 (PBST) three times for 5 minutes each. The sections were then pre-treated with 3% H2O2 in PBST 1% Triton X-100 for 20 minutes to block endogenous peroxidase activity. Following pretreatment, sections were blocked with 2.5% horse serum (Vector Laboratories; #2-2012) for 30 minutes at room temperature. Primary antibodies for GFAP (Sigma; #G3893; 1:500) and IBA1 (Wako; #019-19741; 1:1000) were applied to the sections and then incubated overnight at 4°C. Primary antibodies were removed the following day and sections were washed three times with PBST for 5 minutes each. Sections were then incubated with the appropriate secondary antibody, Immpress HRP Anti-rabbit IgG (Vector Laboratories; #MP-7401) or Immpress HRP Anti-mouse IgG (Vector Laboratories; #MP-7402), for 30 minutes at room temperature on a rocker. After washing twice with PBST for 5 minutes each, sections were treated with NovaRED Peroxidase (HRP) Substrate (Vector Laboratories; #SK-4800) and incubated until the desired stain was achieved. Control sections were incubated with secondary antibodies only. After staining, tissues were carefully mounted on Superfrost plus slides (VWR International: #48311-703) using diH2O and dried in the dark for 1 hour. Coverslips were applied with Vectashield mounting media (Vector Laboratories; #H-1000-10). Immunostained sections were imaged with a digital Olympus microscope and levels of GFAP and IBA1 immunoreactivity were quantified using Image-Pro Plus software (Media Cybernetics, Silver Spring, MD). For each slide, areas of interest in the hippocampus, including CA1, CA2/3, and DG regions, were analyzed to estimate the average intensity of the immunostaining, corrected for background levels obtained from tissue sections processed without primary antibody. The corrected optical density was calculated as follows: corrected optical density = optical density − background.

2.5. Study Population

This study recruited people with HIV (PWH) and people without HIV (PWoH) with varying demographic characteristics (e.g., age, sex). All PWH on stable antiretroviral therapy (ART) for at least six months were considered virally suppressed. Participants were grouped based on their HIV status and cannabis use patterns following recruitment in San Diego, CA, USA. To account for variability in cannabis use characteristics (e.g., frequency, quantity, mode of administration, cannabinoid content), both laboratory measures and self-report questionnaires were used to comprehensively characterize current and lifetime cannabis use. Prior to the assessment, current cannabis users were asked to adhere to their regular use pattern to mitigate potential withdrawal effects. Cannabis use groups were categorized as naive (never used or used ≤6 times/year with ≥ 60 days of abstinence), moderate (one to six uses a week), or daily (seven days a week). In addition to comprehensive medical and neurobehavioral assessments, participants also underwent venous blood collection. Individuals who tested positive for substances other than cannabis were excluded or rescheduled to minimize potentially confounding effects of acute substance use. Additional exclusion criteria include uncontrolled medical, psychiatric, or neurological conditions; a DSM diagnosis of moderate to severe drug use disorder other than cannabis within the past five years, or mild use disorder within the past six months (excluding tobacco); moderate to severe alcohol use disorder within the past 12 months; safety contraindications for MRI; renal insufficiency, which may increase the risk for nephrogenic systemic fibrosis associated with gadolinium-based contrast agents; allergy to gadolinium-based contrast agents; pregnant or breastfeeding. A total of 55 eligible participants (see Table 1) were included in data from this study.

 doi:10.20944/preprints202408.0904.v1

Table 1. Clinical and demographic characteristics of study population. GDS = global deficit score, POMS = Profile of Mood States.

HIV Status	Sex (M/F/TBD)	Ethnicity (% Hispanic)	Race (% White)	Education (years)
HIV-	11 / 3 / 3	14.3	14.3	15.5
HIV+	32 / 4 / 6	13.3	76.7	15.6
Group	**Age (years ± SEM)**	**GDS (score ± SEM)**	**POMS (score ± SEM)**	**Infection Duration (years ± SEM)**
HIV+ Naive (n=22)	63.68 ± 1.69	0.37 ± 0.08	1.78 ± 0.29	27.46 ± 2.25
HIV+ Moderate (n=12)	55.83 ± 3.51	0.46 ± 0.13	2.05 ± 0.52	22.42 ± 2.76
HIV+ Daily (n=8)	53.62 ± 5.19	0.82 ± 0.3	2.55 ± 0.26	28.49 ± 1.91
HIV- Naïve (n=8)	51.75 ± 7.14	0.28 ± 0.05	1.20 ± 0.30	N/A ± N/A
HIV- Moderate (n=1)	29.0 ± N/A	0.06 ± N/A	0.19 ± N/A	N/A ± N/A
HIV- Daily (n=8)	44.0 ± 4.98	0.25 ± N/A	2.94 ± N/A	N/A ± N/A

2.6. Separation and Treatment of Monocyte-Derived Macrophages (MDM)

Peripheral blood mononuclear cell (PBMC) isolation was performed on donor blood by ficoll gradient separation. Briefly, 15 mL of donor blood was slowly layered onto 15mL of HISTOPAQUE-1077 (Sigma Life Sciences; #10771) and centrifuged at 400g for 30 minutes. The monocyte layer was collected, washed with 1X PBS, and centrifuged at 250g before resuspending cells in Iscove's Modified Dulbecco's Medium (IMDM; Gibco; #12440053) supplemented with 10% human serum (Millipore Sigma; #H5667), 1% penicillin/streptomycin (Gibco; #15140122). Automated cell counting was performed on a Countess™ 3 FL (ThermoFisher Scientific; #AMQAF2000) using 0.4% trypan blue solution (Amresco; #K940100ML). Cells were plated in 24-well plates (Corning; #3524) at 400,000 cells/well for RNA testing or 96-well plates (Thermo Scientific; #164588) at 100,000 cells/well for protein testing. Cells were maintained and differentiated in a humidified incubator at 5% CO2 and 37◎C over 7 days before receiving experimental treatment. Monocyte-derived macrophages (MDMs) were pre-treated for one hour with cannabidiol (CBD; Cerilliant Supelco; #C-045; 30 μM) before incubating with IL1β (Invivogen; #6409-44-01; 20 ng/mL) for 6h prior to RNA isolation or 24h prior to fixation and immunostaining. Additional pre-treatments for inhibitor studies include AM 251 (CB1 antagonist; Tocris; #1117; 10 uM), AM 630 (CB2 antagonist; Tocris Bioscience; #1120; 10 uM), GW 6471 (PPARα antagonist; Cayman Chemical; #11697; 10 uM), or GW 9662 (PPARγ antagonist; Cayman Chemical; #70785; 10 uM). Supernatants were collected and MDMs were washed with 1X PBS prior to RNA isolation or fixation with 4% paraformaldehyde (PFA) solution in PBS (Thermo Scientific; #J19943K2).

 doi:10.20944/preprints202408.0904.v1

2.7. Real-Time Quantitative Polymerase Chain Reaction (qPCR) and RNA-Sequencing

RNA isolation was performed according to manufacturer's instructions via Qiagen RNeasy Plus Mini Kit (Qiagen; #74136). Total RNA from MDMs was used for RNA-sequencing and RT-qPCR after being analyzed for purity and concentration with a spectrophotometer. RNA was reverse transcription to cDNA using the High Capacity cDNA Reverse Transcription Kit (Applied Biosystems; #4368814) with the kit provided instructions. Multiplex relative quantification assays were performed on a QuantStudio 3 Real-Time PCR machine (Applied Biosystems; #A28567) using TaqMan Fast Advanced Master Mix for qPCR (Applied Biosystems; #4444557) and individual probes for TREM2 (Hs00219132_m1; #4351370), CHIT1 (Hs00185753_m1; #4448892), SMAD3 (Hs00969210_m1; #4453320), ZAP70 (Hs00896345_m1; #4448892), TREM1 (Hs00218624_m1; #4453320), and VSIG4 (Hs00200695_m1; 4453320). For each assay, ACTB (Applied Biosystems; #4310881E) was used as the endogenous control and fold change in gene expression was quantified via the comparative Ct method, as previously described [62]. All donor samples were run in technical duplicates. RNA-Sequencing was performed at the UC San Diego IGM Genomics Center utilizing an Illumina NovaSeq 6000 that was purchased with funding from a National Institutes of Health SIG grant (#S10 OD026929). The libraries were sequenced on a NovaSeq S4 flow cell, with initial quality control checks, including per-base sequence quality, GC content, and sequence duplication levels conducted using FastQC (v0.11.9). Clean reads were aligned to the hg38 human reference genome using STAR aligner (v2.7.9a) with default parameters on the Illumina BaseSpace Sequence Hub platform. Differential expression analysis was conducted using DESeq2 (v1.30.0) in R (v4.0.5), with genes displaying a false discovery rate (FDR) < 0.05 considered significantly differentially expressed. Gene ontology (GO) and pathway enrichment analyses were performed using PANGEA (v1.1) and identified significantly enriched GO terms and pathways with a corrected p-value < 0.05.

2.8. Enzyme-Linked Immunosorbent Assay (ELISA)

Supernatants collected from treated MDMs were processed to determine levels of sTREM2 using a Human TREM-2 ELISA Kit (Sigma-Aldrich, St. Louis, MO, USA; # RAB1091). Samples were assessed in duplicate and absorbance was measured at 450 nm using a Synergy HTX plate reader (BioTek Instruments Inc., USA).

2.9. Immunocytochemistry for TREM2

Cells were washed twice with 1X PBS and subsequently fixed with PFA (4% w/v) for 20 minutes at 4°C followed by two washes with 1X PBS. The fixed cells were then incubated with blocking buffer (5% BSA, 0.2% Triton-X in 1X PBS) for one hour at room temperature. Primary antibodies for TREM2 (Thermo Scientific; #PA5-87933) were added in blocking buffer (1:250 dilution) and cells were incubated overnight at 4°C. After primary antibody incubation, cells were washed three times with 1X PBS. Alexa Fluor conjugated secondary antibodies (Invitrogen; #A21039) in 1X PBS (1:500 dilution) were then added and incubated for 30 minutes at room temperature on a shaker. Secondary antibodies were removed and cells were washed twice with 1X PBS before being incubated with DAPI solution (Thermo Scientific; #D3571; 1:10,000 dilution in 1X PBS) for 5 minutes. The cells were washed twice then kept in 1X PBS before fluorescent imaging on a CellInsight CX5 HCS Platform (Thermo Scientific; #CX51110).

2.10. Statistical Analysis

All data presented as mean ± SEM with statistical analyses that include one-way and two-way ANOVA with Holm-Sidak post-hoc multiple comparisons tests when appropriate, unless stated otherwise. Statistical significance was determined at $p<0.05$ for all data, with individual p-values reported when near the significance threshold. All sample sizes and data normalizations are listed in figure legends. Data was analyzed on GraphPad Prism 10.0 software (San Diego, CA, USA).

 doi:10.20944/preprints202408.0904.v1

3. Results

3.1. EcoHIV Reduces Levels of TREM2 and Alters Memory in Wildtype and TREM2^{R47H} Mice

First, we utilized WT mice and mice with the R47H loss-of-function mutation to determine if EcoHIV alters TREM2 protein levels. Immunoblot analyses were performed to determine total expression levels of TREM2 in the frontal cortex brain tissue of WT and TREM2^{R47H} mice treated with EcoHIV or saline (Figure 1A). Densitometry analyses for TREM2 protein normalized to ACTB revealed a reduction in total TREM2 in lysates from EcoHIV-infected WT mice, but no difference in lysates from EcoHIV-treated TREM2^{R47H} mice (Figure 1B). When assessing the ratio of intensity between immature and mature bands from TREM2, EcoHIV-treated WT mice had a significantly higher immature:mature isoform ratio compared to saline controls as well as lysates from TREM2^{R47H} mice (Figure 1C). Similarly, the ratio of intensity between bands for the CTF isoform and total TREM2 was significantly higher in EcoHIV-treated WT mice as compared to saline controls and the CTF:TREM2 lysate ratios from TREM2^{R47H} mice (Figure 1D). Collectively, we show that EcoHIV alters the ratio of the different forms of TREM2 in WT but not in mice with a loss-of-function mutation.

To begin assessing the impact of EcoHIV treatment on learning and memory, WT and TREM2^{R47H} mice were placed on a Y-maze for three consecutive days of habituation before a final test 72h after habituation. Total Activity Memory (TAM) testing assessed exploratory behavior, which showed increased beam breaks in EcoHIV-treated WT and TREM2^{R47H} mice compared to saline-treated WT controls (Figure 1E). Total distance traveled during behavioral testing also showed increased activity in EcoHIV-treated WT and TREM2^{R47H} mice compared to saline-treated WT mice (Figure 1F).

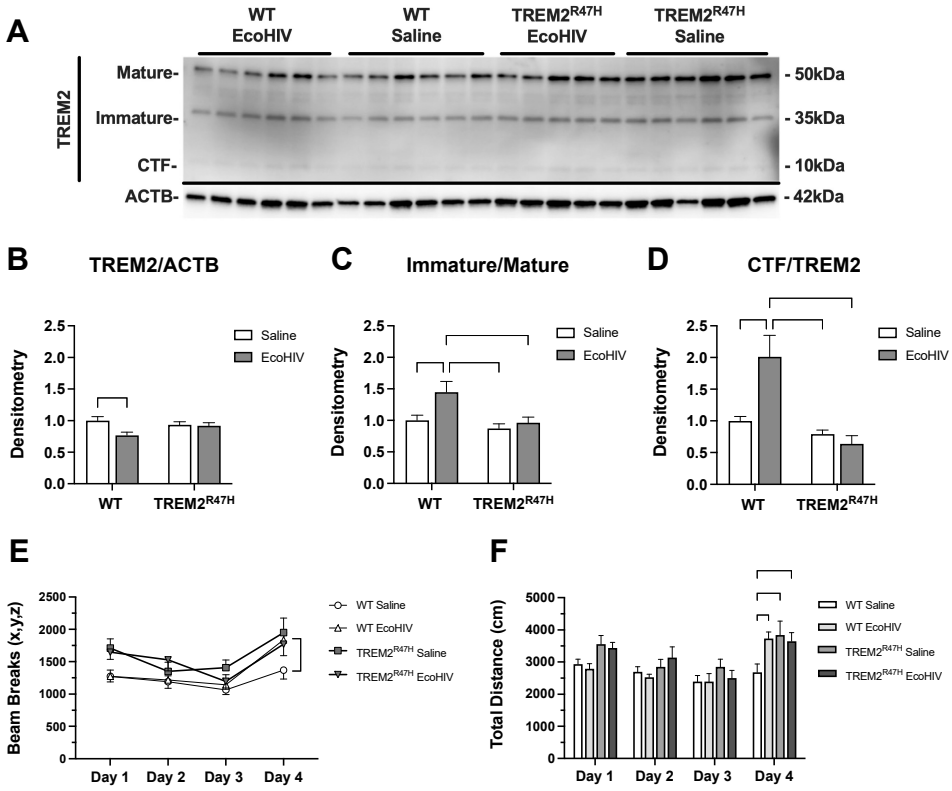

Figure 1. EcoHIV reduces levels of TREM2 and alters learning in TREM2^{R47H} and WT mice. (A) Detection of the mature, immature, carboxy terminal fragment (CTF) isoforms for TREM2 in wild type (WT) and TREM2^{R47H} mice treated with EcoHIV or saline. Densitometry measurement ratios of (B) total TREM2 to ACTB, (C) immature to mature TREM2 isoforms, and (D) CTF to total TREM2 band density. (E) Total Activity Measurements represented as beam breaks over four days in WT and TREM2^{R47H} mice treated with EcoHIV or saline. (F) Total distance traveled during behavioral testing in WT and TREM2^{R47H} mice treated with EcoHIV or saline. Day 4 of behavioral tests occurred 72h

 doi:10.20944/preprints202408.0904.v1

after mice were tested for three consecutive days (Days 1-3). Data represented as mean ± SEM and analyzed using two-way ANOVA with Holm-Sidak's multiple comparisons tests; n=5-6 per condition; *p<0.05, **p<0.01, ***p<0.001.

3.2. EcoHIV Increases Hippocampal IBA1 Expression in TREM2^{R47H} Mice

To evaluate the status of microglial activation following infection with EcoHIV in WT and TREM2^{R47H} mice, we immunostained vibratome sections of mouse brains with antibody for IBA1 using NovaRed for visualization in the hippocampus (HC). Areas analyzed included the whole HC and its following sub-regions: CA1, CA2/3, and dentate gyrus (DG). In whole HC, IBA1 signal was less intense in saline-treated TREM2^{R47H} mice as compared to saline-treated WT mice, and IBA1 signal was more intense in T TREM2^{R47H} mice infected with EcoHIV compared to T TREM2^{R47H} saline control and WT mice (Figure 2A). Quantification of relative optical density revealed a ~71% reduction of IBA1 in saline-treated TREM2^{R47H} mice compared to saline-treated WT mice (Figure 2B). Relative optical density for IBA1 from EcoHIV-treated TREM2^{R47H} mice was ~69% greater than EcoHIV-treated WT mice, and ~582% greater than saline-treated TREM2^{R47H} mice (Figure 2B). In the CA1 region of the HC, IBA1 signal was less intense in saline-treated TREM2^{R47H} mice compared to WT mice and EcoHIV-treated TREM2^{R47H} mice (Figure 2C). Quantification of relative optical density in the CA1 region of saline-treated TREM2^{R47H} mice was decreased by ~73% compared to saline-treated WT controls (Figure 2D). Relative optical density for IBA1 in the CA1 region of the HC from EcoHIV-treated TREM2^{R47H} mice was ~559% greater compared saline-treated TREM2^{R47H} mice (Figure 2D). EcoHIV treatment increased IBA1 levels in CA2/3 region of TREM2^{R47H} mice by 160% and 483% compared to EcoHIV-treated WT and saline-treated TREM2^{R47H} mice, respectively (Figure 2E-F).In the DG region of the HC, IBA1 signal was less intense in saline-treated TREM2^{R47H} mice compared to all other groups (Figure 2G). Quantification of corrected optical density in the DG region showed ~72% reduction in IBA1 in saline-treated TREM2^{R47H} compared to saline-treated WT mice (Figure 2H). Relative optical density for IBA1 in the DG region of EcoHIV-treated TREM2^{R47H} mice was 264%, 290%, and 520% greater than saline-treated WT mice, EcoHIV-treated WT mice, and saline-treated TREM2^{R47H} mice, respectively (Figure 2H). Taken together, EcoHIV increased IBA1 expression in TREM2^{R47H} mice.

 doi:10.20944/preprints202408.0904.v1

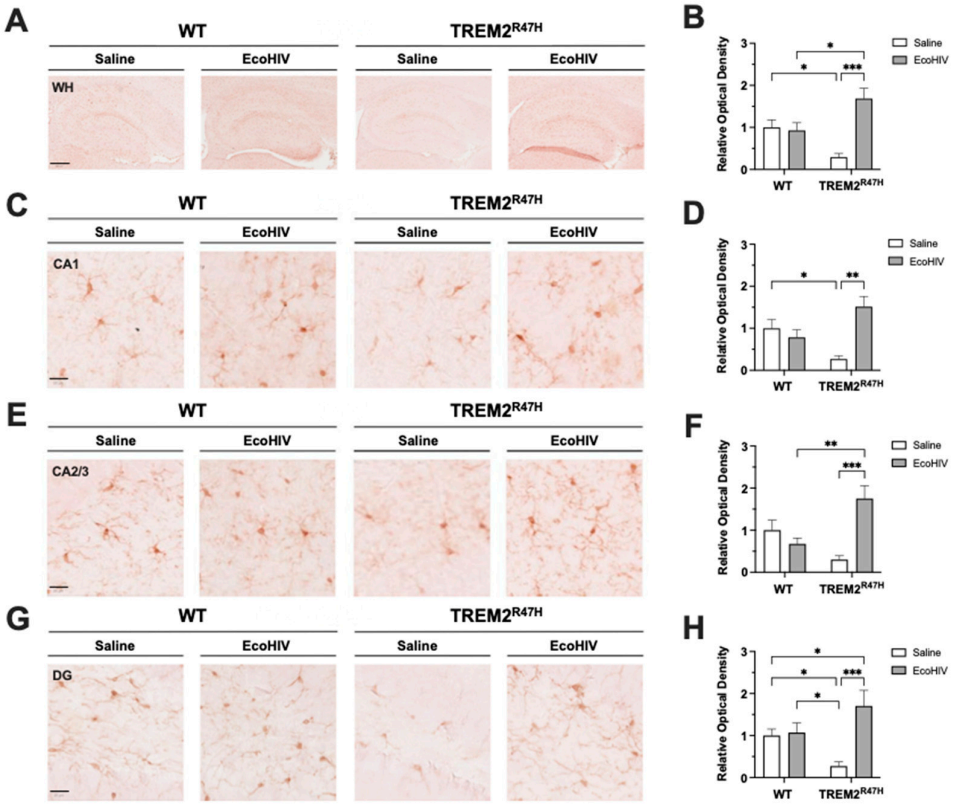

Figure 2. EcoHIV increases hippocampal IBA1 expression in TREM2^{R47H} mice. (A) IBA1 (ionized calcium binding adaptor molecule 1, i.e., microglia) immunostaining of whole hippocampi (400 µm scale bar) for wild type (WT) and TREM2^{R47H} mice. (B) Quantification of relative optical density for whole hippocampi. (C) IBA1 immunostaining of CA1 (20 µm scale bar). (D) Quantification of relative optical density for CA1. (E) IBA1 immunostaining of CA2/3 (20 µm scale bar). (F) Quantification of relative optical density for CA2/3. (G) IBA1 immunostaining of dentate gyrus (DG) (20 µm scale bar). (H) Quantification of relative optical density for DG. Data represented as mean ± SEM and analyzed using two-way ANOVA with Holm-Sidak's multiple comparisons tests; n=5-6 per condition; *p<0.05, **p<0.01, ***p<0.001.

3.3. Hippocampal GFAP Expression Is Increased in TREM2^{R47H} Mice Infected with EcoHIV

Following detection of increased microglia activation, we then explored if this effect was accompanied by increased astrocyte reactivity. To evaluate the status of astroglial activation following EcoHIV infection in WT and TREM2^{R47H} mice, we immunostained vibratome sections of mouse brains with antibody for GFAP using NovaRed for visualization in the HC. Areas analyzed included the whole HC and its following sub-regions: CA1, CA2/3, and DG. In whole HC, GFAP signal was increased by ~186% in EcoHIV-treated TREM2^{R47H} mice as compared to saline-treated TREM2^{R47H} mice as well as EcoHIV-treated WT mice (Figure 3A-B). Relative optical density for GFAP in whole HC from EcoHIV-treated TREM2^{R47H} mice was ~247% greater compared to EcoHIV-treated WT mice (Figure 3B). In the CA1 region of the HC, GFAP signal was less intense in both saline-treated and EcoHIV-treated WT mice compared to EcoHIV-treated TREM2^{R47H} mice (Figure 3C). Quantification of relative optical density in the CA1 region of EcoHIV-treated TREM2^{R47H} mice was ~216% greater than saline-treated WT controls (Figure 3D). Relative optical density for GFAP in the CA1 region of the HC from EcoHIV-treated TREM2^{R47H} mice was also ~245% greater compared EcoHIV-treated WT mice (Figure 3D). In the CA2/3 region of the HC, GFAP signal was more intense in EcoHIV-treated TREM2^{R47H} mice compared to EcoHIV-treated WT mice (Figure 3E). Quantification of relative optical density in the CA2/3 region of the HC from EcoHIV-treated TREM2^{R47H} mice

 doi:10.20944/preprints202408.0904.v1

showed ~226% greater GFAP signal compared to EcoHIV-treated WT mice (Figure 3F). In the DG region of the HC, GFAP signal was less intense in both saline-treated and EcoHIV-treated WT mice when compared to EcoHIV-treated TREM2^{R47H} mice (Figure 3G). Quantification of corrected optical density in the DG region of TREM2^{R47H} mice showed GFAP signal was ~226% greater compared to saline-treated WT mice (Figure 3H). Relative optical density for GFAP in the DG region of EcoHIV-treated TREM2^{R47H} mice was also ~346% greater than EcoHIV-treated WT mice (Figure 3H). Collectively, EcoHIV increased both microglia and astrocyte reactivity in TREM2^{R47H} mice.

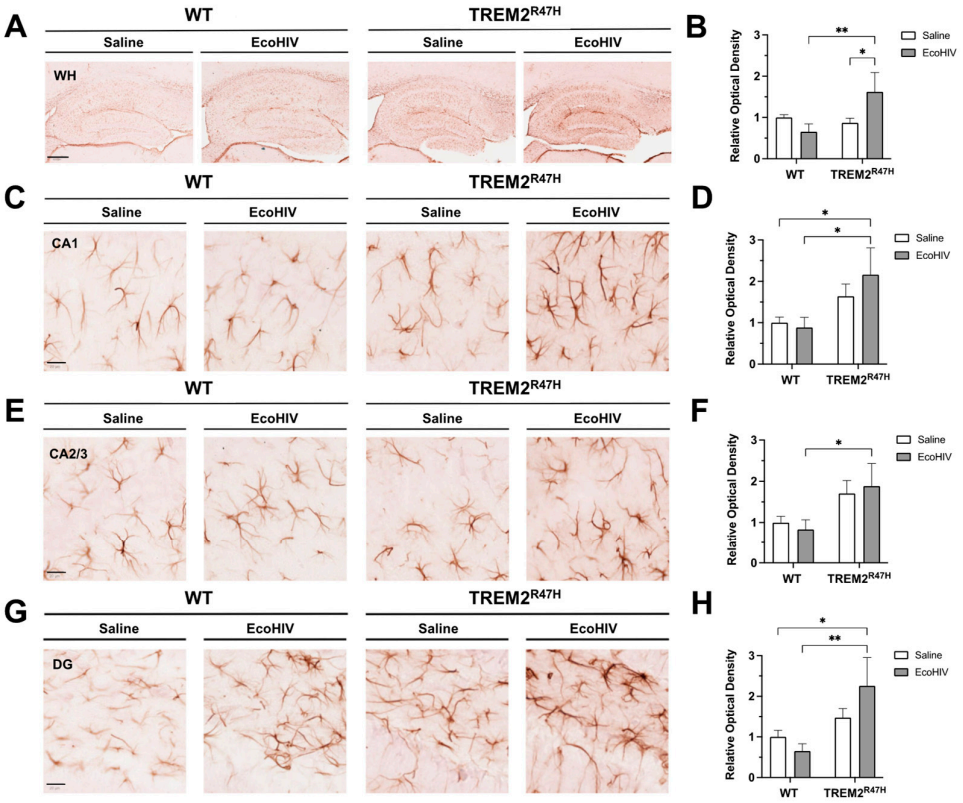

Figure 3. Hippocampal GFAP expression is increased in TREM2^{R47H} mice infected with EcoHIV. (A) GFAP (glial fibrillary acidic protein, i.e., astroglia) immunostaining of whole hippocampi (400 µm scale bar) for wild type (WT) and TREM2R47H mice. (B) Quantification of relative optical density for whole hippocampi. (C) GFAP immunostaining of CA1 (20 µm scale bar). (D) Quantification of relative optical density for CA1. (E) GFAP immunostaining of CA2/3 (20 µm scale bar). (F) Quantification of relative optical density for CA2/3. (G) GFAP immunostaining of dentate gyrus (DG) (20 µm scale bar). (H) Quantification of relative optical density for DG. Data represented as mean ± SEM and analyzed using two-way ANOVA with Fisher's LSD multiple comparisons tests; n=4-6 per condition; *p<0.05, **p<0.01, ***p<0.001.

3.4. The Relationship between TREM2 and Age Is Differentially Affected by Cannabis and HIV

Having established that HIV modulates TREM2 levels and increases glial activity in mice, we further investigated this relationship using ex vivo cultured MDMs. First, we measured TREM2 mRNA in MDMs from PWH and PWoH with varying age and cannabis use frequency (e.g., naïve, moderate, daily). To begin, correlation analyses were performed to assess the relationship between age and TREM2 mRNA levels. In PWoH without cannabis use, we detected a modest positive correlation between TREM2 mRNA and age (p=0.06; r2= 0.60) (Figure 4A). In PWoH with cannabis use, we obsrved a weak positive correlation between TREM2 mRNA and age (p=0.34; r2=0.22) (Figure 4B). No correlation was observed between TREM2 mRNA and age in PWH that do not use cannabis (p=0.62; r2=0.02) (Figure 4C). Contrastingly, in PWH with cannabis use, we detected a significant

 doi:10.20944/preprints202408.0904.v1

inverse correlation between TREM2 mRNA and age (p=0.02; r2=0.35) (Figure 4D). Altogether, correlation analyses indicated TREM2 mRNA levels are associated with age and cannabis use.

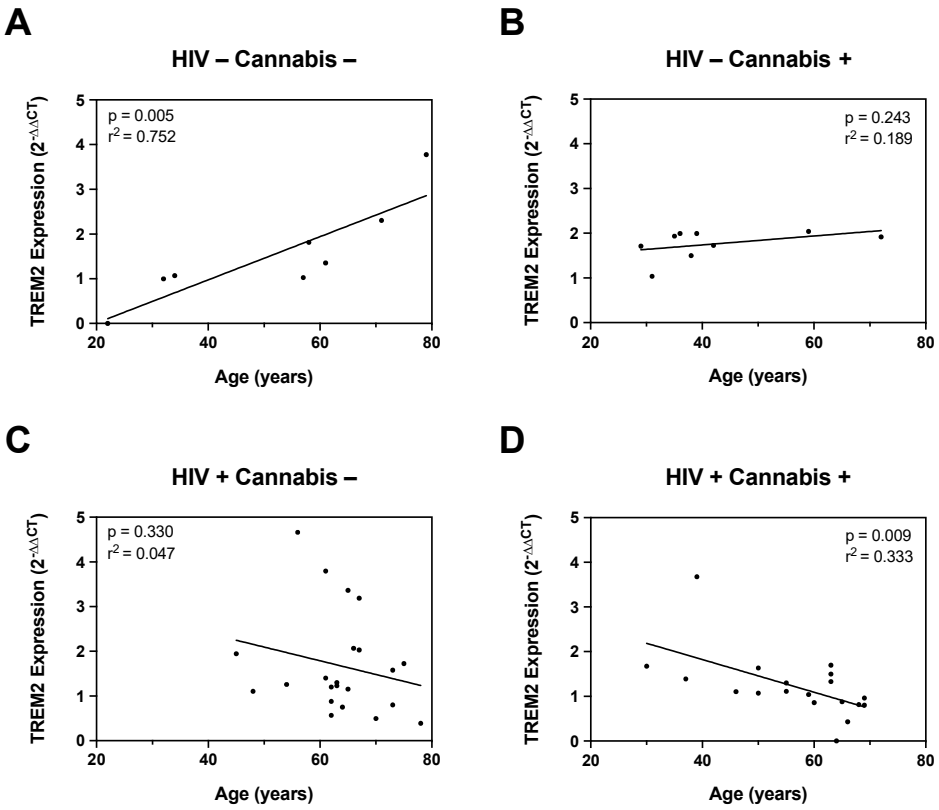

Figure 4. The relationship between monocyte-derived macrophage TREM2 mRNA expression and age is differentially affected by cannabis and HIV. (A) Correlation plot for TREM2 mRNA versus age in HIV- Naïve cannabis users (n=6). (B) Correlation plot for TREM2 mRNA versus age in HIV- Moderate and HIV- Daily cannabis users (n=7). (C) Correlation plot for TREM2 mRNA versus age in HIV+ Naïve cannabis users (n=20). (D) Correlation plot for TREM2 mRNA versus age in HIV+ Moderate and HIV+ Daily cannabis users (n=14). All correlation plots analyzed via simple linear regression.

3.5. TREM2 Expression in MDMs Treated with CBD is Differentially Modulated by Cannabis Use, HIV Status, and Cannabinoid/PPAR Antagonists

To further assess the effects of cannabinoids on TREM2 mRNA, MDMs from HIV- and HIV+ Naïve, Moderate, and Daily cannabis users were treated with CBD in the presence of the inflammatory cytokine IL1B. In HIV- Naive MDMs (Figure 5A), IL1B treatment significantly decreased TREM2 expression by 33.7% compared to vehicle, while CBD treatment resulted in a 33.3% increase. Cotreatment with CBD and IL1B (C+I) increased TREM2 expression by 29.9% relative to IL1B alone. In HIV- Moderate MDMs (Figure 5B), IL1B significantly decreased TREM2 expression by 33.9% whereas CBD increased TREM2 expression by 34.8% compared to vehicle. Compared to IL1B alone, C+I cotreatment resulted in a 30.8% increase in TREM2 expression. In HIV- Daily MDMs (Figure 5C), IL1B treatment decreased TREM2 expression by 34.8% relative to vehicle controls. In contrast, CBD alone resulted in a 7.5% increase, relative to vehicle, while C+I resulted in a 15.2% increased relative to IL1B treatment. In HIV+ Naive MDMs (Figure 5D), IL1B treatment decreased TREM2 expression by 33.4% compared to vehicle controls, while CBD treatment resulted in a 15.0% increase in TREM2 expression. Cotreatment with C+I increased TREM2 expression by 27.6% compared to IL1B alone. For HIV+ Moderate MDMs (Figure 5E), IL1B decreased TREM2 expression by 32.4% compared to vehicle, while CBD only increased TREM2 expression by 6.2%. The C+I

 doi:10.20944/preprints202408.0904.v1

cotreatment resulted in a 7.7% increase in TREM2 expression relative to IL1B alone. In HIV+ Daily MDMs (Figure 5F), IL1B treatment decreased TREM2 expression by 33.2% relative to vehicle controls. CBD treatment resulted in a 3.3% increase in TREM2 expression compared to vehicle, while C+I cotreatment increased TREM2 expression by 25.5% compared to IL1B treatment alone. When comparing HIV- and HIV+ MDMs in the absence of cannabis use (Figure 5G), reduction in TREM2 expression due to IL1B was more pronounced in HIV+ MDMs (42.8%) than in HIV- MDMs (24.8%). Moreover, CBD treatment significantly increased TREM2 expression in HIV- MDMs by 41.6% compared to only 0.9% in HIV+ MDMs. Differences were also noted in response to AM 630 and GW 6471 combined with C+I, with HIV- MDMs showing significantly higher TREM2 expression (23.6% and 32.6%, respectively) compared to HIV+ MDMs. When comparing HIV- and HIV+ MDMs in the presence of cannabis use (Figure 5H), reduction in TREM2 expression due to IL1B was 20.5% greater in HIV+ MDMs than in HIV- MDMs. Cotreatment with C+I led to a significantly larger decrease in TREM2 expression in HIV+ MDMs (28.5%) compared to HIV- MDMs (0.6%). When treated with AM 630, GW 6471, or GW 9662 in combination with C+I, TREM2 expression in HIV+ MDMs compared to HIV- MDMs was significantly greater by 24.2%, 17.5%, and 38.7%, respectively.

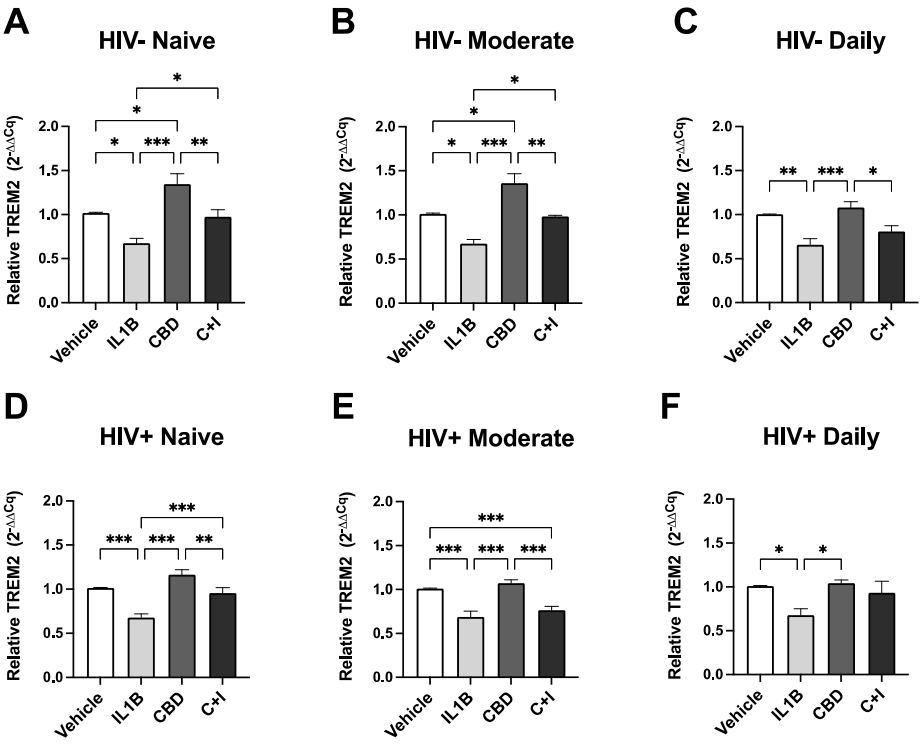

 doi:10.20944/preprints202408.0904.v1

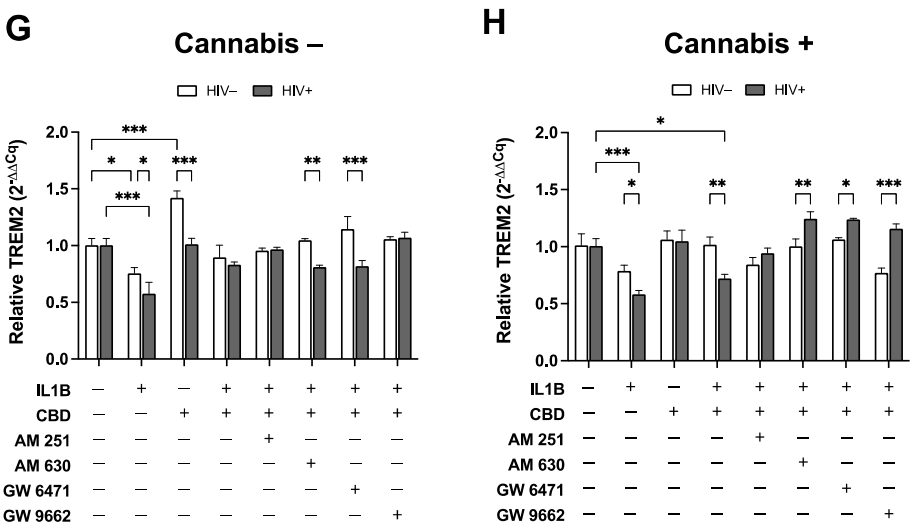

Fig :ed
wi ate
(n= ily
(n= G)
Ca ith
IL1 B1

receptor antagonist; 1 uM, AM 630; CB2 receptor antagonist; 1 uM, GW 6471; PPARα antagonist; 1 uM, and GW 9662; PPARγ antagonist; 1 uM. TREM2 expression levels were measured by qPCR and presented as relative expression (2−ΔΔCq); n=3 per condition. Data represented as mean ± SEM and analyzed using one-way (A-F) and two-way (G-H) ANOVA with Holm-Sidak's multiple comparisons tests. *p<0.05, **p<0.01, ***p<0.001.

3.6. Cannabis Use Is Associated with Altered TREM2 and TREM2-Related mRNA Expression in MDMs Isolated from Blood Samples of HIV Patients

To investigate the associations between HIV and cannabis use with TREM2 and TREM2-related gene expression, RNA was sequenced from MDMs generated from the following four groups: HIV- Naïve, HIV+ Naïve, HIV+ Moderate, and HIV+ Daily. Volcano plots with corresponding gene ontology (GO) terms depict changes in the genetic profile of MDMs isolated from HIV+ Naïve backgrounds. Relative to HIV- Naïve, MDMs from HIV+ Naïve backgrounds displayed a downregulation of genes such as TMEM176B, CHIT1, SERPINF1, TMEM176A, and CXCL10 while upregulation was observed in genes such as DPYSL3, ITGB3, GREM1, TREM1, and MMP12. (Figure 6A, fold change >2, p adj <0.05). Relative to HIV+ Naïve, MDMs from HIV+ Moderate PWH displayed an altered transcriptomic profile with XXX and YYY genes up- and down-regulated, respectively (Figure 6B). Reversed gene expression patterns relative to HIV+ Naïve were seen in MDMs from HIV+ Moderate backgrounds, including upregulation of genes such as TMEM176B, CHIT1, SERPINF1, and TMEM176A as well as a downregulation of genes such as ITGB3, DPYSL3, and GREM1 (Figure 6B). Similar differences in gene expression patterns were seen in MDMs from HIV+ Daily backgrounds, including upregulation of TMEM176B, SERPINF1, and TMEM176A as well as downregulation of ITGB3, GREM1, and MMP12 (Figure 6C). Immune and inflammatory processes were among the top identified biological processes among all cannabis backgrounds (Figure 6A-C).

To reduce the dimensionality of RNA-sequencing data, a principal component analysis (PCA) plot was generated to visualize patterns of variation among CBD-treated MDMs from HIV+ Naïve, HIV+ Moderate, and HIV+ Daily backgrounds (Figure 6D). The two principal components (PC1 and PC2), representing 50% and 46% of the sample variance respectively, illustrate distinct gene expression profiles associated with CBD-treated MDMs from different cannabis use patterns in PWH

 doi:10.20944/preprints202408.0904.v1

(Figure 6D). Additionally, a heat map was generated to further visualize differences in expression of TREM2-related genes in MDMs from HIV- Naïve, HIV+ Naïve, HIV+ Moderate, and HIV+ Daily cannabis use backgrounds (Figure 6E). Further transcriptomic analyses revealed differences in differentially expressed genes, such as CHIT1, SMAD3, ZAP70, TREM1, and VSIG4, in vehicle-treated MDMs from different backgrounds (Figure 6F). MDMs from HIV+ Moderate or HIV+ Daily cannabis use backgrounds showed significant upregulation of the genes CHIT1, SMAD3, and ZAP70 as compared to HIV- Naïve controls, whereas the same genes were significantly downregulated in MDMs from HIV+ Naïve backgrounds as compared to HIV- Naïve controls (Figure 6F). Contrastingly, TREM1 and VSIG4 gene expression in MDMs from HIV+ Moderate and HIV+ Daily cannabis use backgrounds were not altered significantly compared to HIV- negative controls. However, TREM1 and VSIG4 gene expression was significantly upregulated in MDMs from HIV+ Naïve cannabis use backgrounds compared to HIV- negative control (Figure 6F). To further validate the gene expression findings from transcriptomic analyses, RT-qPCR analyses was performed with additional donor samples which revealed comparable patterns in relative gene expression for the genes CHIT1, SMAD3, and VSIG4, (Figure 6G). MDMs from HIV+ Moderate and HIV+ Daily cannabis use backgrounds had ~101% and ~150% increased expression of CHIT1, respectively, relative to MDMs from HIV+ Naïve backgrounds (Figure 6G). Relative to HIV+ Naïve controls, SMAD3 gene expression increased by ~47% and ~161% in MDMs from HIV+ Moderate and HIV+ Daily cannabis use backgrounds, respectively. There were no significant differences in relative expression of ZAP70 and TREM1, however, MDMs from HIV+ Daily backgrounds had a ~112% reduction in relative gene expression of VSIG4 compared to MDMs from HIV+ Naïve backgrounds (Figure 6G).

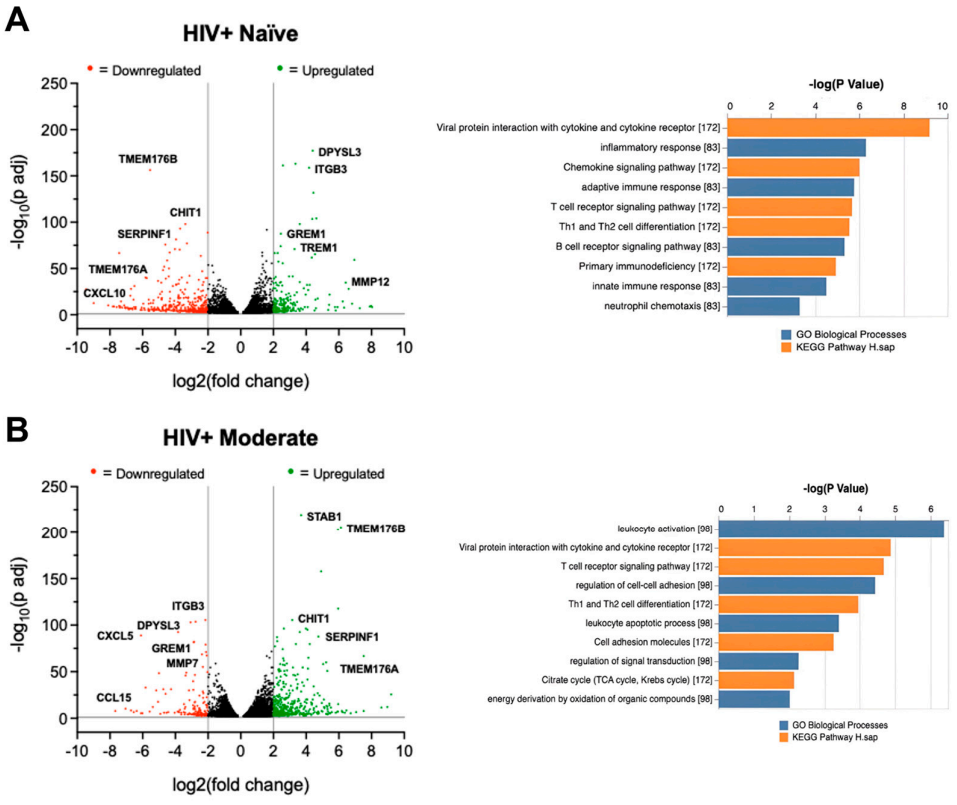

 doi:10.20944/preprints202408.0904.v1

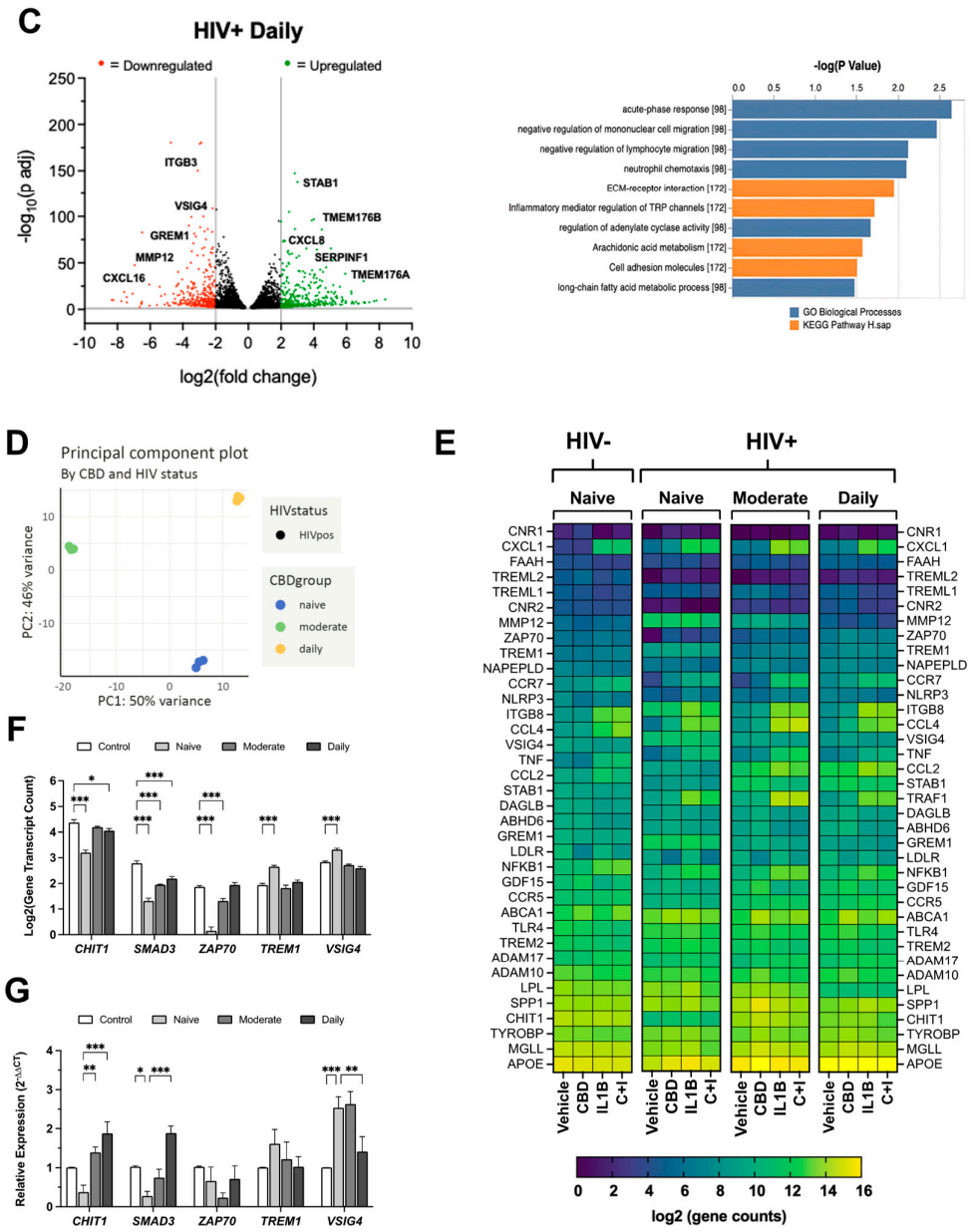

Figure 6. Cannabis use alters TREM2 and TREM2-related mRNA expression in monocyte-derived macrophages (MDMs) isolated from blood samples of people with HIV. Volcano plots with corresponding GO term plots relative to HIV- Naïve for (A) HIV+ Naïve, (B) HIV+ Moderate, and (C) HIV+ Daily patients. (D) Principal component analysis (PCA) plot displaying sample variance among MDMs from people with HIV with varying cannabis use frequency. (E) Heat map of TREM2-related and other relevant genes in MDMs pre-treated with cannabidiol (CBD, 30μM) or vehicle for 1h prior to IL1B (20ng/ml) or vehicle for 6h. C+I = CBD + IL1B (F) Differentially expressed genes from RNAseq and (G) RT-qPCR analysis from additional donor samples. Data represented as mean ± SEM and analyzed using two-way ANOVA with Holm-Sidak's multiple comparisons tests; n=3 per condition; *p<0.05, **p<0.01, ***p<0.001.

3.7. CBD Reduces sTREM2 and Increases Membrane-Bound TREM2 in Cultured MDMs

To determine the effect of CBD on cleavage of TREM2, sTREM2 in media collected from treated MDMs was measured via ELISA. IL1B-treated MDMs had ~45% increased relative absorbance of sTREM2 compared to vehicle controls, and CBD-treated MDMs had the lowest relative absorbance

 doi:10.20944/preprints202408.0904.v1

of sTREM2, compared to vehicle controls (Figure 7A). Although non-significant, cotreatment with CBD and IL1B showed a ~18% decrease in relative absorbance of sTREM2 compared to media collected from IL1B-treated MDMs (Figure 7A). Intensity of membrane-bound TREM2 was significantly reduced in IL1B-treated MDMs (Figure 7B). Quantification of relative TREM2 intensity revealed a ~38% reduction in TREM2 signal from IL1B-treated MDMs relative to vehicle-controls. Cotreatment with CBD and IL1B resulted in significant increase in TREM2 signal relative to IL1B alone and a ~16% decrease in TREM2 signal relative to vehicle controls (Figure 7C).

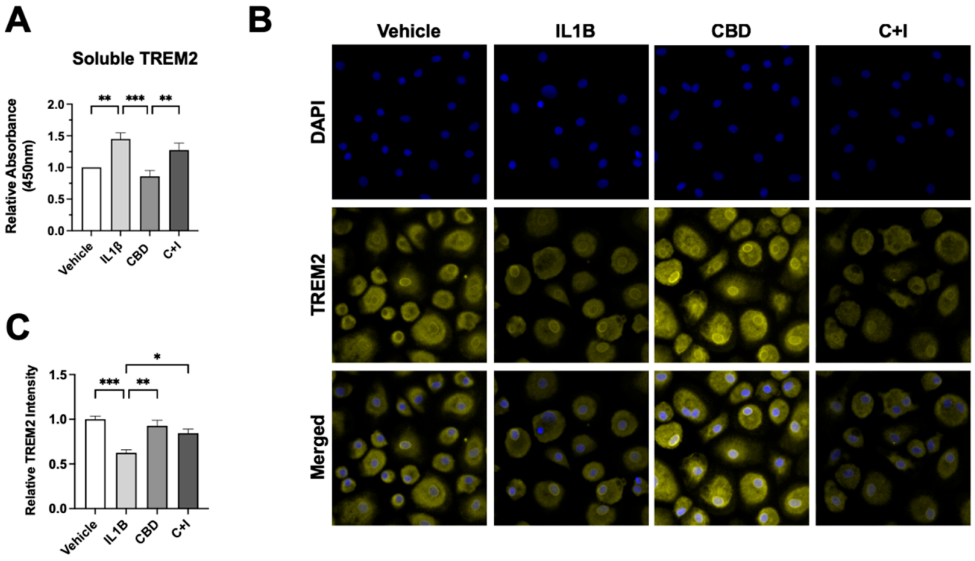

Figure 7. Cannabidiol (CBD) reduces soluble (sTREM2) and increases membrane-bound TREM2 in cultured monocyte-derived macrophages (MDMs). (A) Relative absorbance for sTREM2 measured via ELISA in cultured MDMs treated with IL1B (20ng/ml), CBD (30μM, 1h pre-treatment), or CBD + IL1B (C+I) (B) Representative images of MDMs from HIV+ Naïve background immunostained for membrane-bound TREM2 following 24h treatment with IL1B, CBD, or C+I. (C) Relative TREM2 intensity for immunostained MDMs treated with IL1B, CBD, or C+I. Data represented as mean ± SEM and analyzed using one-way ANOVA with Holm-Sidak's multiple comparisons tests; n=3-6 per condition; *p<0.05, **p<0.01, ***p<0.001.

4. Discussion

In this study, we investigated the relationship between TREM2, age, and HIV-associated neurocognitive impairment as well as evaluated the impact of cannabis use on TREM2 expression and neuroinflammation in PWH. Our observation of decreased total TREM2 expression in response to EcoHIV infection corroborates previous work which shows decreased TREM2 in membrane-enriched fractions of brain homogenates from PWH with HAND [48]. Behavioral analyses revealed significant differences in TAM scoring in EcoHIV-treated WT mice, which performed similarly to TREM2R47H mice independent of EcoHIV or saline treatment. Additionally, alterations in TREM2 expression were accompanied by changes in microglial activation in TREM2 R47H mice, as evidenced by differential IBA1 expression patterns in various hippocampal subregions. Consistent with these findings, other studies have shown that alterations in TREM2 expression can modulate microglial activation and influence cognitive function in various disease models [63,64]. Moreover, gene variants of TREM2, such as R47H TREM2, have also been associated with an increased risk of developing AD [65–68].

In addition to EcoHIV infection, our study also assessed the influence of HIV status, age, and cannabis use on gene expression and TREM2-mediated neuroinflammatory responses. Correlation analyses revealed distinct age-associated changes in TREM2 expression between HIV- and HIV+ individuals, with cannabis use modulating these relationships. Specifically, cannabis use was linked to lower TREM2 mRNA levels in older individuals. These findings are in line with emerging evidence

 doi:10.20944/preprints202408.0904.v1

suggesting bidirectional interactions between cannabinoids and neuroinflammation [69]. While endocannabinoid system has been shown to regulate immune cell function via the cannabinoid type-2 (CB2) receptor, the specific mechanisms underlying the effects of cannabis on TREM2 expression remain unclear and warrant further investigation. Nevertheless, cannabis contains various cannabinoids, such as cannabidiol (CBD) and delta-9-tetrahydrocannabinol (THC), which have been shown to exert anti-inflammatory effects through various mechanisms, including modulation of cytokine production and immune cell function [57]. Notably, CBD has been shown to modulate microglial activation in various disease models, including HIV-associated and Aβ-induced neuroinflammation [57,70–72]. The anti-inflammatory actions of cannabis are largely attributed to cannabinoids which can act on multiple targets within the endocannabinoid system, including the cannabinoid type-2 (CB2) receptor [58,73]. However, CBD has also been shown to exert its effects on microglia through other signaling pathways [74].

The pharmacological agents AM 251, AM 630, GW 6471, and GW 9662 have been utilized to elucidate the roles of cannabinoid receptors and peroxisome proliferator-activated receptors (PPARs) in immunomodulation. AM 251, a selective CB1 receptor antagonist, and AM 630, a CB2 receptor antagonist, are commonly used to block cannabinoid receptor activity. Studies indicate that blocking CB1 and CB2 receptors can influence macrophage polarization and immune response. For example, AM 630 has been shown to alter the anti-inflammatory effects in MDMs, suggesting a role for CB2 in macrophage-mediated immune responses [75]. GW 6471, a PPARα antagonist, and GW 9662, a PPARγ antagonist, are used to investigate the involvement of PPARs in immune cell function. PPARγ, in particular, is known for its role in regulating macrophage activation and inflammation. Inhibition of PPARγ by GW 9662 has been observed to impact macrophage differentiation and inflammatory cytokine production, indicating its regulatory function in immune responses [76].

In contrast, TREM2 exerts its anti-inflammatory effects primarily through modulation of microglial function and the immune response within the CNS. While both CBD and TREM2 may have potential therapeutic implications for neuroinflammatory conditions, they likely act through distinct mechanisms and may target different aspects of the inflammatory cascade. Despite this, cannabis contains hundreds of other phytocannabinoids, terpenoids, and polyphenols that may exert immunomodulatory functions through TREM2-related pathways [71]. Indeed, recent evidence suggests that certain plant-derived compounds exert anti-inflammatory actions on microglial cells via the TREM2 signaling pathway [77]. In human MDMs, treatment with CBD consistently resulted in increased TREM2 mRNA regardless of HIV status or cannabis use frequency. These results indicate that CBD treatment mitigates the IL1B-induced downregulation of TREM2, which has been shown to be induced by inflammatory stimuli [78]. These findings suggest that the immune-modulatory effects of CBD and other cannabinoids are influenced by prior cannabis use and underscore the importance of considering cannabis use history in studies evaluating the therapeutic potential of cannabinoids in individuals with HIV.

In addition to TREM2, HIV-associated changes in gene expression of immunomodulatory genes, including CHIT1[79], SMAD3[80], ZAP70[81], TREM1[82,83], and VISG4[84], were differentially impacted by cannabis use. RNA-sequencing analyses revealed additional differences in the gene expression profile of MDMs from moderate or daily cannabis use backgrounds. This is line with recent findings that illustrate daily cannabis use is associated with lower inflammation in the CNS of PWH [85]. ELISA and immunoblot analyses revealed opposing effects of IL1B and CBD on sTREM2 levels and TREM2 protein expression, highlighting the complex interplay between inflammatory stimuli and cannabinoid signaling pathways. These results suggest that CBD may ameliorate inflammation in part by maintaining TREM2 expression and reducing sTREM2. Additional research is not only necessary to understand the complex molecular makeup of cannabis, but also is imperative to elucidate the potential underlying molecular mechanisms shared by TREM2 and cannabis-derived anti-inflammatory mediators.

While our study provides valuable insights into the role of TREM2 and the potential impact of cannabis on neuroinflammation in HAND, it is essential to acknowledge several limitations that may affect the generalizability and interpretation of our findings. Firstly, our study relied on a limited

 doi:10.20944/preprints202408.0904.v1

number of donors, which may not fully represent the diversity and variability within the population of people living with HIV. Additionally, the age of donors may not encompass the full spectrum of age-related changes that could influence TREM2 expression and neuroinflammatory processes. Moreover, while our analysis revealed alterations in TREM2 expression and neuroinflammatory markers in an EcoHIV-infected mouse model, it is crucial to recognize that this model lacks key components of HIV neuropathogenesis, such as the gp120 protein. Furthermore, our study did not consider the potential effects of antiretroviral therapy (ART) in the mouse model which could significantly influence TREM2 expression, neuroinflammation, and cognition. This line of reasoning may explain the lack of negative effects from the NOR results in EcoHIV-treated mice. Lastly, our study did not explore the effects of minor cannabinoids that are present in cannabis, and these may be responsible for observed associations with reduced inflammation and neuroprotection in PWH. Therefore, while our findings provide valuable insights, further research with larger sample sizes, diverse populations, consideration of age-related changes, inclusion of relevant HIV components, and exploration of therapeutic interventions is warranted to validate and extend our findings.

5. Conclusions

In summary, our study provides novel insights into the intricate relationship between TREM2, neuroinflammation, and cognitive function in the context of HIV infection and cannabis use. First, findings from this murine model highlight the importance of considering genetic susceptibility to TREM2 gene mutations which may further exacerbate the cognitive and behavioral deficits associated with chronic neuroinflammation. Secondly, our ex vivo findings indicate CBD's anti-inflammatory potential to lessen neuroinflammation is linked to changes in both mRNA and protein expression. Altogether, results from this study underscore the potential of TREM2 as a therapeutic target for the treatment of HAND. Further research is warranted to elucidate the specific mechanisms underlying these interactions and to explore potential therapeutic strategies targeting TREM2 and cannabinoid signaling pathways in neuroinflammatory diseases.

References

1. Zenebe, Y., et al., *Worldwide Occurrence of HIV-Associated Neurocognitive Disorders and Its Associated Factors: A Systematic Review and Meta-Analysis.* Front Psychiatry, 2022. **13**: p. 814362.
2. Mekuriaw, B., et al., *Prevalence and variability of HIV/AIDS-associated neurocognitive impairments in Africa: a systematic review and meta-analysis.* BMC Public Health, 2023. **23**(1): p. 997.
3. Nightingale, S., et al., *Cognitive impairment in people living with HIV: consensus recommendations for a new approach.* Nature Reviews Neurology, 2023. **19**(7): p. 424-433.
4. *Diagnoses of HIV Infection in the United States and Dependent Areas 2019: National Profile*, in *HIV Surveillance Report*, C.f.D.C.a. Prevention, Editor. 2021.
5. Alakkas, A., et al., *White matter damage, neuroinflammation, and neuronal integrity in HAND.* J Neurovirol, 2019. **25**(1): p. 32-41.
6. Keledjian, K., et al., *Correlation of HIV-Induced Neuroinflammation and Synaptopathy with Impairment of Learning and Memory in Mice with HAND.* J Clin Med, 2023. **12**(16).
7. Solomon, I.H., et al., *White Matter Abnormalities Linked to Interferon, Stress Response, and Energy Metabolism Gene Expression Changes in Older HIV-Positive Patients on Antiretroviral Therapy.* Mol Neurobiol, 2020. **57**(2): p. 1115-1130.
8. Mackiewicz, M.M., et al., *Pathogenesis of age-related HIV neurodegeneration.* J Neurovirol, 2019. **25**(5): p. 622-633.
9. Lopez Angel, C.J., et al., *Signatures of immune dysfunction in HIV and HCV infection share features with chronic inflammation in aging and persist after viral reduction or elimination.* Proc Natl Acad Sci U S A, 2021. **118**(14).
10. Silvin, A., J. Qian, and F. Ginhoux, *Brain macrophage development, diversity and dysregulation in health and disease.* Cell Mol Immunol, 2023. **20**(11): p. 1277-1289.
11. Koenig, S., et al., *Detection of AIDS virus in macrophages in brain tissue from AIDS patients with encephalopathy.* Science, 1986. **233**(4768): p. 1089-93.
12. Gu, C.J., et al., *EcoHIV infection of mice establishes latent viral reservoirs in T cells and active viral reservoirs in macrophages that are sufficient for induction of neurocognitive impairment.* PLoS Pathog, 2018. **14**(6): p. e1007061.
13. Potash, M.J., et al., *A mouse model for study of systemic HIV-1 infection, antiviral immune responses, and neuroinvasiveness.* Proc Natl Acad Sci U S A, 2005. **102**(10): p. 3760-5.

 doi:10.20944/preprints202408.0904.v1

14. Kim, B.-H., et al., *EcoHIV Infection of Primary Murine Brain Cell Cultures to Model HIV Replication and Neuropathogenesis.* Viruses, 2024. **16**(5): p. 693.
15. Burdo, T.H., A. Lackner, and K.C. Williams, *Monocyte/macrophages and their role in HIV neuropathogenesis.* Immunol Rev, 2013. **254**(1): p. 102-13.
16. Fields, J.A., et al., *Alterations in brain TREM2 and Amyloid-beta levels are associated with neurocognitive impairment in HIV-infected persons on antiretroviral therapy.* J Neurochem, 2018.
17. Fields, J., et al., *Age-dependent molecular alterations in the autophagy pathway in HIVE patients and in a gp120 tg mouse model: reversal with beclin-1 gene transfer.* J Neurovirol, 2013. **19**(1): p. 89-101.
18. Guha, D., et al., *CSF Extracellular Vesicle Abeta42 and Tau/Abeta42 Ratio Are Associated with Cognitive Impairment in Older People with HIV.* Viruses, 2023. **16**(1).
19. Porcheray, F., et al., *Macrophage activation and human immunodeficiency virus infection: HIV replication directs macrophages towards a pro-inflammatory phenotype while previous activation modulates macrophage susceptibility to infection and viral production.* Virology, 2006. **349**(1): p. 112-20.
20. Ye, L., et al., *IL-1beta and TNF-alpha induce neurotoxicity through glutamate production: a potential role for neuronal glutaminase.* J Neurochem, 2013. **125**(6): p. 897-908.
21. Jay, T.R., V.E. von Saucken, and G.E. Landreth, *TREM2 in Neurodegenerative Diseases.* Mol Neurodegener, 2017. **12**(1): p. 56.
22. Li, Y., et al., *TREM2 Regulates High Glucose-Induced Microglial Inflammation* via *the NLRP3 Signaling Pathway.* Brain Sci, 2021. **11**(7).
23. Zhu, Z., et al., *TREM2 suppresses the proinflammatory response to facilitate PRRSV infection* via *PI3K/NF-kappaB signaling.* PLoS Pathog, 2020. **16**(5): p. e1008543.
24. Li, C., et al., *TREM2 inhibits inflammatory responses in mouse microglia by suppressing the PI3K/NF-κB signaling.* Cell Biol Int, 2019. **43**(4): p. 360-372.
25. Rivest, S., *TREM2 enables amyloid beta clearance by microglia.* Cell Res, 2015. **25**(5): p. 535-6.
26. Jin, S.C., et al., *TREM2 is associated with increased risk for Alzheimer's disease in African Americans.* Mol Neurodegener, 2015. **10**: p. 19.
27. Lue, L.F., et al., *TREM2 Protein Expression Changes Correlate with Alzheimer's Disease Neurodegenerative Pathologies in Post-Mortem Temporal Cortices.* Brain Pathol, 2015. **25**(4): p. 469-80.
28. Yeh, F.L., et al., *TREM2 Binds to Apolipoproteins, Including APOE and CLU/APOJ, and Thereby Facilitates Uptake of Amyloid-Beta by Microglia.* Neuron, 2016. **91**(2): p. 328-40.
29. Colonna, M. and Y. Wang, *TREM2 variants: new keys to decipher Alzheimer disease pathogenesis.* Nat Rev Neurosci, 2016. **17**(4): p. 201-7.
30. Kobayashi, M., et al., *TREM2/DAP12 Signal Elicits Proinflammatory Response in Microglia and Exacerbates Neuropathic Pain.* J Neurosci, 2016. **36**(43): p. 11138-11150.
31. Henjum, K., et al., *Cerebrospinal fluid soluble TREM2 in aging and Alzheimer's disease.* Alzheimers Res Ther, 2016. **8**(1): p. 17.
32. Zheng, H., et al., *TREM2 Promotes Microglial Survival by Activating Wnt/beta-Catenin Pathway.* J Neurosci, 2017. **37**(7): p. 1772-1784.
33. Zhong, L., et al., *Soluble TREM2 induces inflammatory responses and enhances microglial survival.* J Exp Med, 2017. **214**(3): p. 597-607.
34. Raha, A.A., et al., *Neuroprotective Effect of TREM-2 in Aging and Alzheimer's Disease Model.* J Alzheimers Dis, 2017. **55**(1): p. 199-217.
35. Foley, J.F., *sTREM2 and neuroinflammation.* Sci Signal, 2017. **10**(470).
36. Le Page, A., et al., *Role of the peripheral innate immune system in the development of Alzheimer's disease.* Exp Gerontol, 2018. **107**: p. 59-66.
37. Morris, J.C. and A.L. Price, *Pathologic correlates of nondemented aging, mild cognitive impairment, and early-stage Alzheimer's disease.* J Mol Neurosci, 2001. **17**(2): p. 101-18.
38. Nixon, R.A., *Autophagy, amyloidogenesis and Alzheimer disease.* J Cell Sci, 2007. **120**(Pt 23): p. 4081-91.
39. Dinkins, C., J. Arko-Mensah, and V. Deretic, *Autophagy and HIV.* Semin Cell Dev Biol, 2010. **21**(7): p. 712-8.
40. Hult, B., et al., *Neurobiology of HIV.* Int Rev Psychiatry, 2008. **20**(1): p. 3-13.
41. Gisslen, M., et al., *CSF concentrations of soluble TREM2 as a marker of microglial activation in HIV-1 infection.* Neurol Neuroimmunol Neuroinflamm, 2019. **6**(1): p. e512.
42. Walter, J., *The Triggering Receptor Expressed on Myeloid Cells 2: A Molecular Link of Neuroinflammation and Neurodegenerative Diseases.* J Biol Chem, 2016. **291**(9): p. 4334-41.
43. Knight, A.C., et al., *Differential regulation of TREM2 and CSF1R in CNS macrophages in an SIV/macaque model of HIV CNS disease.* J Neurovirol, 2020. **26**(4): p. 511-519.
44. Azzolini, F., et al., *Neuroinflammation Is Associated with GFAP and sTREM2 Levels in Multiple Sclerosis.* Biomolecules, 2022. **12**(2).
45. La Rosa, F., et al., *TREM2 Expression and Amyloid-Beta Phagocytosis in Alzheimer's Disease.* Int J Mol Sci, 2023. **24**(10).

 doi:10.20944/preprints202408.0904.v1

46. Jonsson, T., et al., *Variant of TREM2 associated with the risk of Alzheimer's disease.* N Engl J Med, 2013. **368**(2): p. 107-16.
47. Tran, K.M., et al., *A Trem2(R47H) mouse model without cryptic splicing drives age- and disease-dependent tissue damage and synaptic loss in response to plaques.* Mol Neurodegener, 2023. **18**(1): p. 12.
48. Fields, J.A., et al., *Alterations in brain TREM2 and Amyloid-beta levels are associated with neurocognitive impairment in HIV-infected persons on antiretroviral therapy.* J Neurochem, 2018. **147**(6): p. 784-802.
49. Abrams, D.I., et al., *Cannabis in painful HIV-associated sensory neuropathy: a randomized placebo-controlled trial.* Neurology, 2007. **68**(7): p. 515-21.
50. Rizzo, M.D., et al., *HIV-infected cannabis users have lower circulating CD16+ monocytes and IFN-gamma-inducible protein 10 levels compared with nonusing HIV patients.* AIDS, 2018. **32**(4): p. 419-429.
51. Manuzak, J.A., et al., *Heavy Cannabis Use Associated With Reduction in Activated and Inflammatory Immune Cell Frequencies in Antiretroviral Therapy-Treated Human Immunodeficiency Virus-Infected Individuals.* Clin Infect Dis, 2018. **66**(12): p. 1872-1882.
52. Ellis, R.J., et al., *Recent cannabis use in HIV is associated with reduced inflammatory markers in CSF and blood.* Neurol Neuroimmunol Neuroinflamm, 2020. **7**(5).
53. Liu, Z., et al., *Cannabis Use Associates With Reduced Proviral Burden and Inflammatory Cytokine in Tissues From Men With Clade C HIV-1 on Suppressive Antiretroviral Therapy.* J Infect Dis, 2024.
54. Watson, C.W., et al., *Cannabis Exposure is Associated With a Lower Likelihood of Neurocognitive Impairment in People Living With HIV.* J Acquir Immune Defic Syndr, 2020. **83**(1): p. 56-64.
55. Ellis, R.J., et al., *Beneficial Effects of Cannabis on Blood-Brain Barrier Function in Human Immunodeficiency Virus.* Clin Infect Dis, 2021. **73**(1): p. 124-129.
56. Esposito, G., et al., *Cannabidiol* in vivo *blunts beta-amyloid induced neuroinflammation by suppressing IL-1beta and iNOS expression.* Br J Pharmacol, 2007. **151**(8): p. 1272-9.
57. Esposito, G., et al., *Cannabidiol reduces Aβ-induced neuroinflammation and promotes hippocampal neurogenesis through PPARγ involvement.* PLoS One, 2011. **6**(12): p. e28668.
58. Borgonetti, V., et al., *Non-psychotropic Cannabis sativa L. phytocomplex modulates microglial inflammatory response through CB2 receptors-, endocannabinoids-, and NF-κB-mediated signaling.* Phytother Res, 2022. **36**(5): p. 2246-2263.
59. Mammana, S., et al., *Could the Combination of Two Non-Psychotropic Cannabinoids Counteract Neuroinflammation? Effectiveness of Cannabidiol Associated with Cannabigerol.* Medicina (Kaunas), 2019. **55**(11).
60. Turcotte, C., et al., *The CB 2 receptor and its role as a regulator of inflammation.* Cell Mol Life Sci, 2016. **73**(23): p. 4449-4470.
61. Rizzo, M.D., et al., *Targeting Cannabinoid Receptor 2 on Peripheral Leukocytes to Attenuate Inflammatory Mechanisms Implicated in HIV-Associated Neurocognitive Disorder.* J Neuroimmune Pharmacol, 2020. **15**(4): p. 780-793.
62. Schmittgen, T.D. and K.J. Livak, *Analyzing real-time PCR data by the comparative C(T) method.* Nat Protoc, 2008. **3**(6): p. 1101-8.
63. Wang, Y., et al., *TREM2 lipid sensing sustains the microglial response in an Alzheimer's disease model.* Cell, 2015. **160**(6): p. 1061-71.
64. Jay, T.R., et al., *Disease Progression-Dependent Effects of TREM2 Deficiency in a Mouse Model of Alzheimer's Disease.* J Neurosci, 2017. **37**(3): p. 637-647.
65. Giraldo, M., et al., *Variants in triggering receptor expressed on myeloid cells 2 are associated with both behavioral variant frontotemporal lobar degeneration and Alzheimer's disease.* Neurobiol Aging, 2013. **34**(8): p. 2077.e11-8.
66. Guerreiro, R., et al., *TREM2 variants in Alzheimer's disease.* N Engl J Med, 2013. **368**(2): p. 117-27.
67. Do, T.H., et al., *TREM2 macrophages induced by human lipids drive inflammation in acne lesions.* Sci Immunol, 2022. **7**(73): p. eabo2787.
68. Olufunmilayo, E.O. and R.M.D. Holsinger, *Variant TREM2 Signaling in Alzheimer's Disease.* J Mol Biol, 2022. **434**(7): p. 167470.
69. Swinton, M.K., et al., *Alterations in Brain Cannabinoid Receptor Levels Are Associated with HIV-Associated Neurocognitive Disorders in the ART Era: Implications for Therapeutic Strategies Targeting the Endocannabinoid System.* Viruses, 2021. **13**(9).
70. Vallée, A., et al., *Effects of cannabidiol interactions with Wnt/β-catenin pathway and PPARγ on oxidative stress and neuroinflammation in Alzheimer's disease.* Acta Biochim Biophys Sin (Shanghai), 2017. **49**(10): p. 853-866.
71. Marini, S., et al., *Oral Cannabidiol Treatment Is Associated with an Anti-Inflammatory Gene Expression Signature in Myeloid Cells of People Living with HIV.* Cannabis Cannabinoid Res, 2024.
72. Tito, P.A.L., et al., *Cannabidiol prevents lipopolysaccharide-induced sickness behavior and alters cytokine and neurotrophic factor levels in the brain.* Pharmacol Rep, 2021. **73**(6): p. 1680-1693.
73. Yndart Arias, A., et al., *Anti-inflammatory effects of CBD in human microglial cell line infected with HIV-1.* Sci Rep, 2023. **13**(1): p. 7376.
74. Yang, S., et al., *Cannabidiol Enhances Microglial Beta-Amyloid Peptide Phagocytosis and Clearance* via *Vanilloid Family Type 2 Channel Activation.* Int J Mol Sci, 2022. **23**(10).

 doi:10.20944/preprints202408.0904.v1

75. Choi, S.M., et al., *Classical monocyte-derived macrophages as therapeutic targets of umbilical cord mesenchymal stem cells: comparison of intratracheal and intravenous administration in a mouse model of pulmonary fibrosis.* Respiratory Research, 2023. **24**(1): p. 68.
76. Feng, D., et al., *Monocyte-derived macrophages orchestrate multiple cell-type interactions to repair necrotic liver lesions in disease models.* The Journal of Clinical Investigation, 2023. **133**(15).
77. Leri, M., et al., *EVOO Polyphenols Exert Anti-Inflammatory Effects on the Microglia Cell through TREM2 Signaling Pathway.* Pharmaceuticals (Basel), 2023. **16**(7).
78. Liu, W., et al., *Trem2 promotes anti-inflammatory responses in microglia and is suppressed under pro-inflammatory conditions.* Hum Mol Genet, 2020. **29**(19): p. 3224-3248.
79. Yu, X., et al., *Chitotriosidase attenuates brain inflammation* via *HDAC3/NF-κB pathway in D-galactose and aluminum-induced rat model with cognitive impairments.* Neuroscience Research, 2021. **172**: p. 73-79.
80. Yim, L.Y., et al., *Transforming Growth Factor β Signaling Promotes HIV-1 Infection in Activated and Resting Memory CD4(+) T Cells.* J Virol, 2023. **97**(5): p. e0027023.
81. Hung, C.-H., et al., *HIV-1 Nef Assembles a Src Family Kinase-ZAP-70/Syk-PI3K Cascade to Downregulate Cell-Surface MHC-I.* Cell Host & Microbe, 2007. **1**(2): p. 121-133.
82. Campbell, G.R., R.K. To, and S.A. Spector, *TREM-1 Protects HIV-1-Infected Macrophages from Apoptosis through Maintenance of Mitochondrial Function.* mBio, 2019. **10**(6).
83. Campbell, G.R., et al., *HIV-1 Tat Upregulates TREM1 Expression in Human Microglia.* J Immunol, 2023. **211**(3): p. 429-442.
84. Li, J., et al., *VSIG4 inhibits proinflammatory macrophage activation by reprogramming mitochondrial pyruvate metabolism.* Nat Commun, 2017. **8**(1): p. 1322.
85. Watson, C.W., et al., *Daily Cannabis Use is Associated With Lower CNS Inflammation in People With HIV.* J Int Neuropsychol Soc, 2021. **27**(6): p. 661-672.